Quantitative Analysis of OCT Characteristics in Patients with Achromatopsia and Blue-Cone Monochromatism

Daniel Barthelmes, Florian K. Sutter, Malaika M. Kurz-Levin, Martina M. Bosch, Horst Helbig, Günter Niemeyer, and Johannes C. Fleischhauer

Purpose. To quantify optical coherence tomography (OCT) images of the central retina in patients with blue-cone monochromatism (BCM) and achromatopsia (ACH) compared with healthy control individuals.

Methods. The study included 15 patients with ACH, 6 with BCM, and 20 control subjects. Diagnosis of BCM and ACH was established by visual acuity testing, morphologic examination, color vision testing, and Ganzfeld ERG recording. OCT images were acquired with the Stratus OCT 3 (Carl Zeiss Meditec AG, Oberkochen, Germany). Foveal OCT images were analyzed by calculating longitudinal reflectivity profiles (LRPs) from scan lines. Profiles were analyzed quantitatively to determine foveal thickness and distances between reflectivity layers.

Results. Patients with ACH and BCM had a mean visual acuity of 20/200 and 20/60, respectively. Color vision testing results were characteristic of the diseases. The LRPs of control subjects yielded four peaks (P1–P4), presumably representing the RPE (P1), the ovoid region of the photoreceptors (P2), the external limiting membrane (ELM) (P3), and the internal limiting membrane (P4). In patients with ACH, P2 was absent, but foveal thickness (P1–P4) did not differ significantly from that in the control subjects (187 ± 20 vs. 192 ± 14 μm, respectively). The distance from P1 to P3 did not differ significantly (78 ± 10 vs. 82 ± 5 μm) between ACH and controls subjects. In patients with BCM, P3 was lacking, and P2 advanced toward P1 compared with the control subjects (32 ± 6 vs. 48 ± 4 μm). Foveal thickness (153 ± 16 μm) was significantly reduced compared with that in control subjects and patients with ACH.

Conclusions. Quantitative OCT image analysis reveals distinct patterns for controls subjects and patients with ACH and BCM, respectively. Quantitative analysis of OCT imaging can be useful in differentiating retinal diseases affecting photoreceptors. Foveal thickness is similar in both normal subjects and patients with ACH but is decreased in patients with BCM. (*Invest Ophthalmol Vis Sci.* 2006;47:1161–1166) DOI:10.1167/iovs.05-0783

Optical coherence tomography (OCT) is an emerging diagnostic technique that allows noninvasive visualization of tissue morphology with high resolution.[1,2] The technique has been established as an important diagnostic tool in various fields of medicine[3–6] and has had a high impact on the diagnosis of various retinal diseases. OCT image analysis is mainly performed qualitatively by pattern recognition on the image acquired. Quantitative analysis of reflectivity of OCT images has been used occasionally to correlate reflectivity patterns with histology in chicken[7] or to observe and quantify changes in retinal reflectivity patterns in animal models or rare human retinal diseases.[8–11]

Cone diseases, such as achromatopsia (ACH) and blue-cone monochromatism (BCM), are often difficult to distinguish in the clinical routine. Sophisticated diagnostic tools are necessary, such as specialized ERG recording protocols, not standardized by the International Society of Clinical Electrophysiology of Vision (ISCEV), or special color vision tests. OCT imaging may offer the possibility of facilitating diagnosis or of classifying patients based on morphologic data. ACH and BCM are diseases affecting cone cells only. The potential of quantitative analysis of OCT images was evaluated in these two entities. Cones have been described to be morphologically present in histologic cross sections of the foveal area in patients with ACH,[12,13] but they obviously lack functional properties. We were able to demonstrate that reflectivity profiles of OCT scans of the fovea allow distinction and quantification of even subtle morphologic differences, not recognizable with currently used analysis methods. OCT imaging will be applicable beyond its current use with our analysis algorithm. Reflectivity profile analysis of in vivo high-resolution OCT images may allow the establishment of new classification criteria for cone diseases.

Materials and Methods

Patients

Control subjects and patients with ACH and BCM underwent slit lamp examination, determination of best corrected visual acuity (BCVA; Snellen and Early Treatment Diabetic Retinopathy Study [ETDRS]), color vision (Farnsworth Panel D-15) testing and Berson's test for BCM.[14] Full-field ERG recordings (UTAS 3000; LKC Technologies Inc., Gaithersburg, MD) were performed according to ISCEV standard protocols.[15] Exclusion criteria were any other accompanying ocular disease, such as other macular diseases or retinal dystrophies; macular edema; diabetic retinopathy; inflammatory disorders; or increased intraocular pressure. Diagnosis of ACH and BCM was established using ERG results, BCVA, and color plate tests (Table 1). All study patients had nystagmus to various degrees. Details are noted in Table 2. Three families (one with six members, two with two members) having ACH were included, the remaining being sporadic cases. In the group of patients with BCM, two families were included (one family with four members, the other with two). The control group consisted of 20 healthy individuals who were not related and were age matched to subjects in the patient groups.

The study was performed in accordance with the tenets of the Declaration of Helsinki 1975 (1983 revision).

Image Acquisition

OCT scanning was performed with Stratus OCT 3 software, version 4.0.1 (Carl Zeiss Meditec AG, Oberkochen, Germany). Ten OCT images

From the Department of Ophthalmology, University Hospital Zurich, Zurich, Switzerland.

Supported by the Paul Schiller Foundation, Zurich, Switzerland.

Submitted for publication June 22, 2005; revised October 19, 2005; accepted January 23, 2006.

Disclosure: **D. Barthelmes**, None; **F.K Sutter**, None; **M.M. Kurz-Levin**, None; **M.M. Bosch**, None; **H. Helbig**, None; **G. Niemeyer**, None; **J.C. Fleischhauer**, None

The publication costs of this article were defrayed in part by page charge payment. This article must therefore be marked "*advertisement*" in accordance with 18 U.S.C. §1734 solely to indicate this fact.

Corresponding author: Johannes C. Fleischhauer, Department of Ophthalmology, University Hospital Zurich, Frauenklinikstrasse 24, CH-8091 Zurich, Switzerland; johannes.fleischhauer@usz.ch.

TABLE 1. Summarized Clinical Data of the Participants

	Control	ACH	BCM
n	20	15	6
Age, y (mean ± SD)	34.7 ± 12.8	27.2 ± 11.0	33.2 ± 20.0
BCVA (EDTRS)	89.7 ± 2.4	41.4 ± 3.7	53.0 ± 6.5
Panel D-15	No pathology	Diffuse error	Tetartan error
Berson Test	Passed	Not passed	Passed
Nystagmus	−	+++	+
Rod-driven ERG response	Normal	Normal	Normal
Cone-driven ERG response	Normal	Absent or severely impaired	Extremely reduced

of the central retina were recorded in each patient. Radially oriented scans with a scan length of 6 mm (standard macular thickness map scan protocol of the OCT software) were used. Sections through the fovea were used for image analysis. To increase the probability of scanning through the center of the fovea, a large amount of repetitive images were recorded (average number of OCT images recorded per patient, 120 ± 12). Ten images were chosen from the total recorded, in which the foveola was precisely cross-sectioned. Parafoveal cross sections can be recognized by the structural changes and hence the changes in reflectivity pattern of the foveola. In addition, the infrared fundus image was used to ensure that the recordings were performed within the foveal region. For further image analysis, 8-bit images were exported. Grayscale images were exported with the built-in export function of the OCT Stratus software and were kept constant for all individuals. Image format was JPG with a color depth of 8-bit (256 grayscale values). Images were used as exported for analysis and not changed in brightness or contrast. Both parameters are preset by the algorithm of the OCT software.

Image Analysis

Detailed image analysis was performed in the foveola (cone cells only, total width of cross sections analyzed was 0.18 mm). Image analysis was performed using ImageJ (http://www.rsb.info.nih.gov/ij/ available developed by Wayne Rasband, National Institutes of Health, Bethesda, MD). Within this selected area, 20 longitudinal reflectivity profiles (LRPs), arranged in a cross-sectional parallel manner, were calculated (see Fig. 3B). An average LRP from the 20 profiles was calculated for each of the 10 OCT scans recorded (IGOR Pro 5.03; WaveMetrics Inc., Lake Oswego, OR), as shown in Figure 3C. An overall average LRP was calculated for every patient from the 10 OCT images recorded. To compare groups, we calculated summary average profiles for ACH, BCM, and the control groups.

Statistical Analysis

Parametric (unpaired *t*-test, ANOVA) and nonparametric (Mann-Whitney, Kruskal-Wallis) test were used (Instat 3.02 software; Graphpad Inc., San Diego, CA). Statistical significance was defined as $P \leq 0.05$.

RESULTS

Clinical evaluation of our study cohort enabled clear differentiation between patients with ACH and BCM and control subjects (Tables 1, 2). Mean age did not differ significantly between the different groups. Visual acuity was significantly lower in patients with ACH or BCM than in controls subjects

TABLE 2. Detailed Clinical Data of the Participants

	ACH Group									
Patient	**1**	**2**	**3**	**4**	**5**	**6**	**7**	**8**	**9**	**10**
ERG signals (ISCEV Standard)										
Scotopic	Normal	Normal	Normal	Normal	Normal	Normal	Normal	Normal	Normal	Normal
Photopic	Severely reduced	Severely reduced	Absent	Absent	Absent	Severely reduced	Absent	Absent	Absent	Absent
VA	20/200	20/200	20/200	20/200	20/200	20/200	20/200	20/200	20/200	20/200
Berson's test	Failed	Failed	Failed	Failed	Failed	Failed	Failed	Failed	Failed	Failed
OCT										
P1 present	Yes	Yes	Yes	Yes	Yes	Yes	Yes	Yes	Yes	Yes
P2 present	No	No	No	No	No	No	No	No	No	No
P3 present	Yes	Yes	Yes	Yes	Yes	Yes	Yes	Yes	Yes	Yes
P4 present	Yes	Yes	Yes	Yes	Yes	Yes	Yes	Yes	Yes	Yes
P1–P2 [μm]	—	—	—	—	—	—	—	—	—	—
P1–P3 [μm]	80.3	89.2	81.1	76.3	84.4	73.0	73.8	65.7	77.1	73.0
P1–P4 [μm]	205.3	208.5	193.9	199.6	171.2	176.1	201.2	178.5	180.9	187.4
Morphological findings										
Foveal reflex	Present	Present	Broadend	Slightly broadend	Present	Present	Present	Broadend	Slightly broadend	Present
Biomicroscopic fundus abnormalities	None	None	None	None	None	None	None	None	None	None
Anterior segement morphology	Normal	Normal	Normal	Normal	Normal	Normal	Normal	Normal	Normal	Normal
Nystagmus	++	+++	+	++	+++	++	++	++	+++	+++

* Mean visual acuity was 20/15, and minimal VA was 20/20. All control subjects had ERG recordings within normal ranges, and all passed Berson's color plate test. In LRPs of OCT images all peaks were present. Numerical values for distances are expressed as the mean ± SD. Biomicroscopic testing revealed no abnormalities in the anterior and posterior segments.

($P < 0.001$). Results of color tests showed the characteristics for ACH and BCM. Nystagmus was more pronounced in patients with ACH than in those with BCM. Rod-driven ERGs were not different within the three groups, whereas cone-driven ERGs were severely reduced or absent in patients with ACH or BCM.

Analysis of OCT images in patients with ACH and BCM (Figs. 1E, 1F) revealed clearly distinguishable reflection profiles in the two disorders (Figs. 2B, 2C). Patients' profiles differed clearly from those of control subjects (Fig. 2D).

Control Subjects

OCT scans through a normal foveola showed four clearly distinguishable, highly reflective bands (peak (P)1–P4; Fig. 1D). These highly reflective bands have been presumed to be (from vitreous to sclera) the internal limiting membrane (P4), the external limiting membrane (P3), the layer between the inner and outer segments of photoreceptors (P2), and the RPE (P1).[16–18] LRPs of normal healthy control subjects (Fig. 3) yielded four distinctive peaks that represent the highly reflective bands (Fig. 2A). LRPs and the four peaks were highly reproducible inter- as well as intraindividually and showed very narrow 99% confidence intervals for intensities and distances (shaded regions around the LRPs in Fig. 2). Assuming P1 represents the RPE and P4 the internal limiting membrane, foveal thickness (distance from P1 to P4) measured 192 ± 14 μm.

Positive Control Group

To verify whether nystagmus affects LRPs, we examined two patients with nystagmus due to alcoholic encephalopathy. Their LRPs were comparable to those of the control subjects. There was no obvious change in foveal reflectivity induced by nystagmus compared with that in the controls subjects.

Patients with ACH

In ACH, reflectivity profiles appeared similar to control profiles, but P2 was missing. Foveal thickness (distance from P1 to P4) and the position of P3 (presumably the external limiting membrane) did not differ significantly from that in control individuals (Fig. 2; $P > 0.05$). Histologic sections of some eyes with ACH[12,13,19] revealed results comparable to the measured foveal thickness (Fig. 4A).

Patients with BCM

Foveal thickness in patients with BCM was significantly reduced compared with that in control individuals and patients with ACH (Fig. 4A; $P < 0.001$). P2 was significantly less reflective ($P < 0.001$) and showed a reduced distance from P1 (RPE) compared with that in controls subjects ($P < 0.0001$). P3 (the external limiting membrane) was missing (Fig. 2).

LRPs and their respective peaks (Fig. 2), resulted in a one-to-one configuration (an unmistakable result) for each group.

Discussion

Distinct profiles for the two cone diseases (BCM and ACH) were calculated with the method of longitudinal reflectivity profile analysis of OCT images. Although these diseases are clinically difficult to distinguish, our analysis algorithm allows reliable and simple differentiation by using the LRPs that yield a one-to-one configuration.

Misinterpretation of profiles is highly unlikely because of the narrow 99% confidence interval. Because of the marked differences and the high reproducibility of LRPs, it is possible to differentiate the two diseases based on the LRP only.

Achromatopsia is a rare congenital retinal disease characterized by an almost absent cone function[20] and is usually inherited in an autosomal recessive manner. Responsible mutations such as CNGA3, CNGB3, and GNAT2[21–25] have been

ACH Group					BCM Group						Control Group*
11	12	13	14	15	1	2	3	4	5	6	(n = 20)
Normal	Normal	Normal	Normal	Normal	Normal	Normal	Normal	Normal	Normal	Normal	Normal
Severely reduced	Severely reduced	Absent	Absent	Severely reduced	Severely reduced	Severely reduced	Severely reduced	Severely reduced	Severely reduced	Severely reduced	Normal
20/200	20/200	20/200	20/200	20/250	20/100	20/66	20/65	20/65	20/40	20/66	20/15
Failed	Failed	Failed	Failed	Failed	Passed	Passed	Passed	Passed	Passed	Passed	Passed
Yes	Yes	Yes	Yes	Yes	Yes	Yes	Yes	Yes	Yes	Yes	Yes
No	No	No	No	No	Yes	Yes	Yes	Yes	Yes	Yes	Yes
Yes	Yes	Yes	Yes	Yes	No	No	No	No	No	No	Yes
Yes	Yes	Yes	Yes	Yes	Yes	Yes	Yes	Yes	Yes	Yes	Yes
—	—	—	—	—	29.7	34.5	34.1	32.9	34.1	30.0	50.5 ± 1.3
71.4	80.3	73.8	76.3	74.6	—	—	—	—	—	—	84.0 ± 1.2
188.8	176.9	174.4	189.9	169.8	146.9	146.9	143.8	155.0	170.0	157.8	202.6 ± 8.2
Present	Marked	Present	Marked	Slightly broadend	Present	Present	Present	Present	Present	Present	Present
None	None	None	None	None	None	None	None	None	None	None	None
Normal	Normal	Normal	Normal	Normal	Normal	Normal	Normal	Normal	Normal	Normal	Normal
+++	++	+	++	++	+++	++	++	+	+	+	—

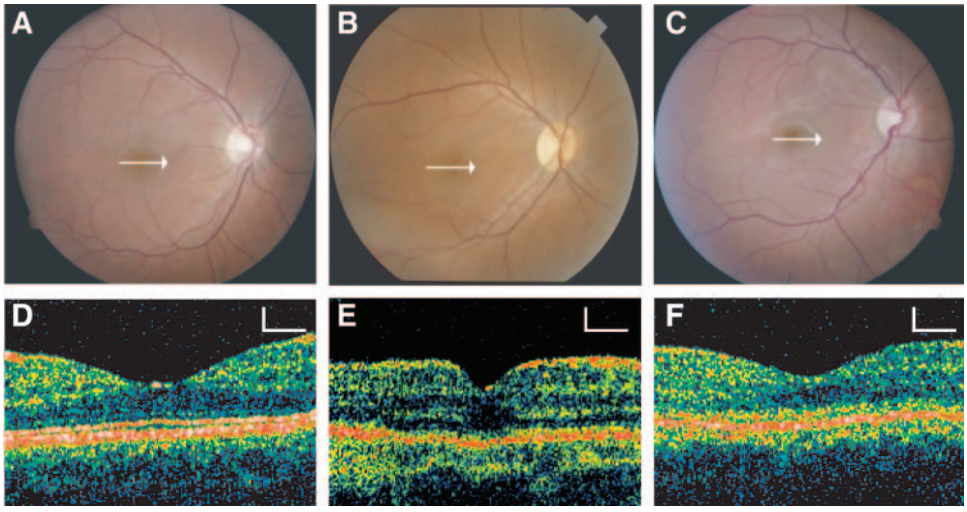

FIGURE 1. Fundus photographs and corresponding OCT images of a normal control subject (**A**, **D**), a patient with ACH (**B**, **E**), and a patient with BCM (**C**, **F**). No obvious pathologic changes are visible. Color differences are due to different imaging techniques. *Arrows* on fundus images: scan direction of corresponding OCT images. Patients with ACH and BCM show apparent changes in thickness and structure in the foveal region. OCT images are all equally sized. There is a change in reflectivity within the parafoveal area in the patient with ACH. This change has not been quantified. Scale bar: vertical, 100 μm; horizontal, 500 μm.

found in several genes. In some patients, an exact chromosomal localization of the mutated gene has not been established yet (e.g., ACHM1).[26] A dysfunction of cones due to these mutations has been proposed as the reason for visual impairment.[21] Patients with ACH usually present with severely impaired visual acuity, a relative central scotoma, congenital nystagmus, and absence of color discrimination. Biomicroscopy shows normal anterior and posterior segment morphology (Fig. 1b) and sometimes a reduced foveal reflex or fine pigment mottling. Visual function in ACH is stationary, and all clinical findings are already present at birth (congenital functional defect of cone system). Falls et al.[12] estimated the number of foveal cones to be normal, whereas extrafoveal cones seemed to be reduced in number. Retinal and foveal thickness were reported to be normal.[12,19] In contrast, the quantity of rods seemed to be normal throughout the entire retina. Foveal cones showed an abnormal configuration of the inner segment as well as dislocated nuclei. Ganzfeld electroretinogram (ERG) findings are described as characteristic for ACH.[27]

On OCT images of patients with ACH, P2 (photoreceptor reflectivity) disappeared completely, whereas histologic examinations have shown that photoreceptors are present.[12] Peak 2 presumably represents a highly reflective structure between the inner and outer photoreceptor segments. This structure may represent the ovoid region of the photoreceptors. The ovoid lies in the outermost part of the inner segment of the photoreceptor and contains densely packed mitochondria. Published reports on histology of eyes with ACH date back to 1921 and 1965, a time before the availability of electron microscopy that can show the presence or absence of mitochondria in the diseased cones. It is tempting to speculate that the missing P2 in OCT scans of patients with ACH

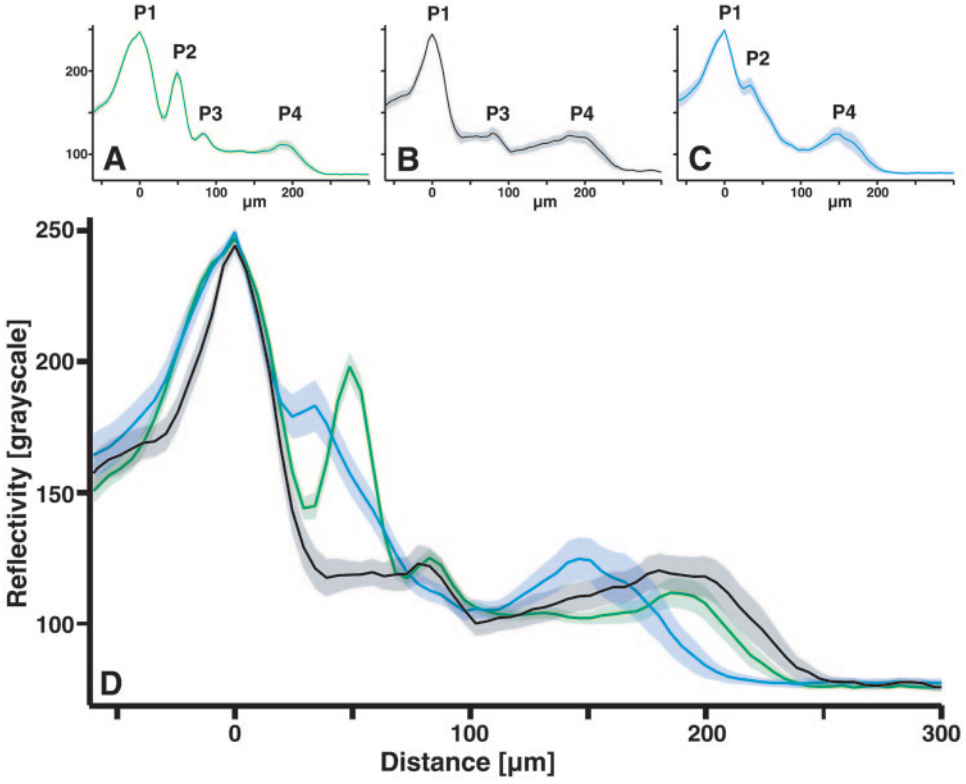

FIGURE 2. The average LRP of (**A**) 20 control subjects, (**B**) 15 patients with ACH, and (**C**) 6 with BCM. (**D**) An overlay of the three LRPs shows the obvious difference in reflectivity within the foveola. Grayscale values, 0–255. *Shaded areas*: 99% CI.

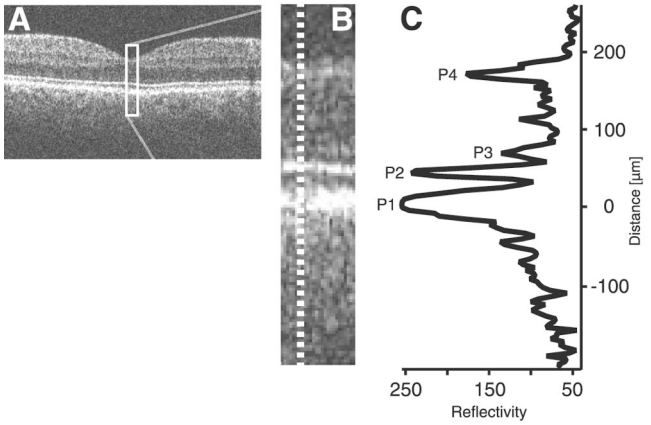

FIGURE 3. Data extraction from grayscale images. (**A**) Complete 8-bit image of control person's macula. (**B**) Enlarged extract from the ROI (foveal region) in (**A**). *Dashed line*: line scan from which the single reflectivity profile (**C**) was calculated. (**C**) Four distinct peaks within the LRP were easily detected. Reflectivity is in 0–255 levels of gray (*x*-axis); scan depth is in micrometers (*y*-axis).

reflects alterations in this mitochondria-rich region of the photoreceptors.

BCM is usually a stationary, X-linked, recessively inherited disease that occurs even less frequently than ACH. However, recent reports indicate that there is evidence of progressive loss of cone function in older individuals.[28,29] Mutations in the red and green opsin genes have been identified (OPN1LW,[30] OPN1MW[31]). Patients with BCM usually have better visual acuity than do patients affected by ACH, and nystagmus often regresses eventually. Despite the reduced cone function, affected persons have a residual ability to distinguish colors—especially shades of blue—used in specific color vision tests.[14] Much as in ACH, biomicroscopy of patients with BCM reveals a normal retinal aspect (Fig. 1C). The ganzfeld ERG shows similar findings as it does for ACH.[32,33] Until now, no histopathological data on BCM have been reported. Clinical distinction between ACH and BCM is difficult, especially in children (Fig. 1). Although BCM is clinically well defined, BCVA, Ganzfeld ERG, and color testing are needed to establish a diagnosis. The method of LRP analysis of OCT images complements the diagnostic procedure, revealing high specificity and reproducibility. The finding that P2 (photoreceptors) is shifted toward P1 (RPE) and reflectivity is significantly reduced indicates a reduction in size of the photoreceptors and a structural modification either of the cell itself or of intracellular organelles (mitochondria). The lack of P3 (external limiting membrane) supports the thesis that a structural change in the photoreceptors and/or surrounding tissue is present. P2 cannot be misinterpreted as P3 because the external limiting membrane never reaches the reflectivity of P2 and the advancement of P2 toward P1 can clearly be seen in all patients (Fig. 1F). Unfortunately, these findings cannot be correlated to morphologic observations, because histologic data of patients with BCM are lacking. Foveal thickness was reduced in patients with BCM compared with those with ACH and controls subjects ($P < 0.001$).

With reference to the progressive forms of BCM with increasing loss of cone function,[28,29] a potential misinterpretation with other forms of progressive maculopathy such as Stargardt's disease could be hypothesized. Besides the phenotypical differences, LRPs in Stargardt's diseases cannot be misinterpreted for BCM. LRPs of patients with Stargardt's disease show only P1 and P4. Peaks 2 and 3 are missing, and foveal thickness is dramatically reduced (~20 μm; Barthelmes D, Fleischhauer JC, unpublished observation, 2005).

We speculate that mutations resulting in the phenotype of BCM lead to a reduction in the size of the photoreceptors (reduced foveal thickness, distance from P1 to P4) and to an alteration of the area between inner and outer photoreceptor segments (shifting of P2 toward P1, absence of P3). These results indicate an alteration of the outer segment of the photoreceptors (shifting of P2 toward P1). The distance from P2 to P4 was less in patients with BCM (121 $\pm$ 10 μm) than that in normal subjects (148 $\pm$ 8 μm). This difference would indicate an alteration in the area of the somata of the photoreceptors. Again, unfortunately no histologic reports are available on BCM to support this hypothesis.

Reports in the literature on foveal thickness measured with OCT devices range from 146 to 153 μm.[3,34,35] These values were acquired by using the built-in algorithm of the OCT software. Because we propose P2 to represent the photoreceptors and P1 the RPE, the standard OCT software calculates foveal thickness from P2 to P4. Already published values are in accordance with ours if the additional ~50 μm from P1 to P2 is added.[3,34,35]

The method of using LRPs to analyze OCT images has primarily been described by Huang et al.[7] In a recent publication, Ishikawa et al.[36] used LRPs to reevaluate retinal thickness in normal and glaucomatous eyes in the macular area.[36] In both studies, the original data sets recorded by the instrument were used to evaluate the reflectivity. In the study by Huang et al.,[36] OCT-1 was used (Carl Zeiss Meditec, AG), which has a much lower resolution (~25 μm) than the newer versions and indeed, LRP revealed much more information on the layerlike structure in the tissue. Ishikawa et al.[36] used the original scan data exported from the Stratus OCT-3 to compare changes in the different retinal layers between control subjects and patients who had glaucoma. For glaucomatous eyes, significant changes in the retinal ganglion cell layer were detected. We

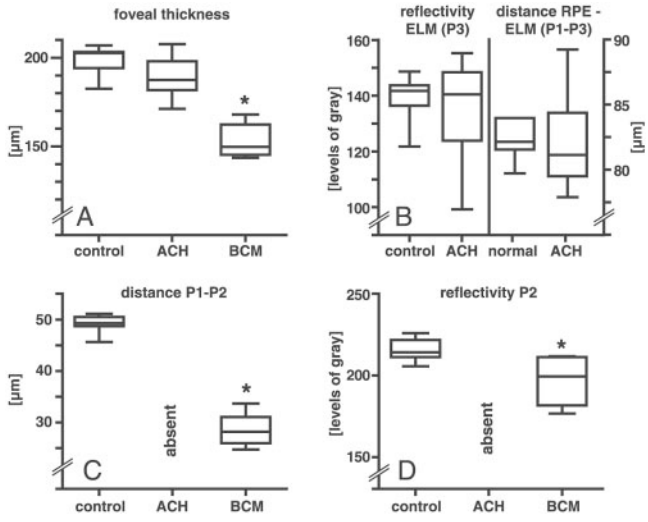

FIGURE 4. Statistical data analysis. (**A**) Foveal thickness in patients with ACH was not significantly different from that in control subjects; patients with BCM showed a statistically significant foveal thinning compared with controls subjects and patients with ACH ($P < 0.001$). (**B**) Reflectivity and distance data of P3 (external limiting membrane; ELM). *Left*: reflectivity of ELM; *right*: distances from the RPE to the ELM (no statistically significant difference). LRPs of patients with BCM did not show ELM reflectivity. (**C**) Distance from P1 to P2 (presumed mitochondria-rich region of the inner photoreceptor segments). In ACH, P2 was not detectable. Distance to P1 (RPE) was significantly different in patients with BCM compared with controls subjects ($P < 0.0001$). (**D**) Reflectivity of P2. In patients with ACH, P2 was not detectable. In those with BCM, reflectivity was significantly lower than in controls subjects ($P < 0.001$). *Statistically significant difference.

exported 8-bit grayscale images for analysis in our approach. Patients with cone disorders often exhibit nystagmus that can be more or less pronounced. Nystagmus makes image acquisition very difficult, especially if there is a need for the fovea to be well discriminated on the images. Off-line analysis of distorted images due to eye movements is much easier if performed on the 8-bit grayscale image, where the region of interest (ROI) can be chosen arbitrarily. Thus, the original A-scans do not have to be selected within the large raw data file itself.

In conclusion, we demonstrate a method to analyze OCT images quantitatively. Two cone diseases were investigated that showed clinically high similarity. They exhibited characteristic features of tissue reflectivity and thus were easily distinguished by longitudinal reflectivity profiles of OCT image analysis.

References

1. Fercher AF. Optical coherence tomography. *J Biomed Opt*. 1996; 1:157–173.
2. Huang D, Swanson EA, Lin CP, et al. Optical coherence tomography. *Science*. 1991;254:1178–1181.
3. Hee MR, Puliafito CA, Wong C, et al. Quantitative assessment of macular edema with optical coherence tomography. *Arch Ophthalmol*. 1995;113:1019–1029.
4. Hee MR, Puliafito CA, Wong C, et al. Optical coherence tomography of macular holes. *Ophthalmology*. 1995;102:748–756.
5. Marghoob AA, Swindle LD, Moricz CZ, et al. Instruments and new technologies for the in vivo diagnosis of melanoma. *J Am Acad Dermatol*. 2003;49:777–797; quiz 98–99.
6. Tearney GJ, Brezinski ME, Bouma BE, et al. In vivo endoscopic optical biopsy with optical coherence tomography. *Science*. 1997; 276:2037–2039.
7. Huang Y, Cideciyan AV, Papastergiou GI, et al. Relation of optical coherence tomography to microanatomy in normal and rd chickens. *Invest Ophthalmol Vis Sci*. 1998;39:2405–2416.
8. Cideciyan AV, Jacobson SG, Aleman TS, et al. In vivo dynamics of retinal injury and repair in the rhodopsin mutant dog model of human retinitis pigmentosa. *Proc Natl Acad Sci USA*. 2005;102: 5233–5238.
9. Huang Y, Cideciyan AV, Aleman TS, et al. Optical coherence tomography (OCT) abnormalities in rhodopsin mutant transgenic swine with retinal degeneration. *Exp Eye Res*. 2000;70:247–251.
10. Jacobson SG, Cideciyan AV, Aleman TS, et al. Crumbs homolog 1 (CRB1) mutations result in a thick human retina with abnormal lamination. *Hum Mol Genet*. 2003;12:1073–1078.
11. Jacobson SG, Sumaroka A, Aleman TS, et al. Nuclear receptor NR2E3 gene mutations distort human retinal laminar architecture and cause an unusual degeneration. *Hum Mol Genet*. 2004;13: 1893–1902.
12. Falls HF, Wolter JR, Alpern M. Typical total monochromacy: a histological and psychophysical study. *Arch Ophthalmol*. 1965;74: 610–616.
13. Larsen H. Demonstration mikroskopischer Präparate von einem monochromatischen Auge. *KlinMbl Augenheilk*. 1921;67:301–302.
14. Berson EL, Sandberg MA, Rosner B, Sullivan PL. Color plates to help identify patients with blue cone monochromatism. *Am J Ophthalmol*. 1983;95:741–747.
15. Marmor MF, Zrenner E. Standard for clinical electroretinography (1999 update). International Society for Clinical Electrophysiology of Vision. *Doc Ophthalmol*. 1998;97:143–156.
16. Yamada E. Some structural features of the fovea centralis in the human retina. *Arch Ophthalmol*. 1969;82:151–159.
17. Drexler W, Sattmann H, Hermann B, et al. Enhanced visualization of macular pathology with the use of ultrahigh-resolution optical coherence tomography. *Arch Ophthalmol*. 2003;121:695–706.
18. Fujimoto JG, Brezinski ME, Tearney GJ, et al. Optical biopsy and imaging using optical coherence tomography. *Nat Med*. 1995;1: 970–972.
19. Glickstein M, Heath GG. Receptors in the monochromat eye. *Vision Res*. 1975;15:633–636.
20. Pokorny J, Smith VC, Pinckers AJ, Cozijnsen M. Classification of complete and incomplete autosomal recessive achromatopsia. *Graefes Arch Clin Exp Ophthalmol*. 1982;219:121–130.
21. Johnson S, Michaelides M, Aligianis IA, et al. Achromatopsia caused by novel mutations in both CNGA3 and CNGB3. *J Med Genet*. 2004;41:e20.
22. Kellner U, Wissinger B, Kohl S, Kraus H, Foerster MH. Molecular genetic findings in patients with congenital cone dysfunction: mutations in the CNGA3, CNGB3, or GNAT2 genes [in German]. *Ophthalmologe*. 2004;101:830–835.
23. Kohl S, Baumann B, Broghammer M, et al. Mutations in the CNGB3 gene encoding the beta-subunit of the cone photoreceptor cGMP-gated channel are responsible for achromatopsia (ACHM3) linked to chromosome 8q21. *Hum Mol Genet*. 2000;9:2107–2016.
24. Kohl S, Baumann B, Rosenberg T, et al. Mutations in the cone photoreceptor G-protein alpha-subunit gene GNAT2 in patients with achromatopsia. *Am J Hum Genet*. 2002;71:422–425.
25. Kohl S, Varsanyi B, Antunes GA, et al. CNGB3 mutations account for 50% of all cases with autosomal recessive achromatopsia. *Eur J Hum Genet*. 2005;13:302–308.
26. Pentao L, Lewis RA, Ledbetter DH, Patel PI, Lupski JR. Maternal uniparental isodisomy of chromosome 14: association with autosomal recessive rod monochromacy. *Am J Hum Genet*. 1992;50: 690–699.
27. Heckenlively JR. Cone dystrophies and dysfunction. In: Heckenlively JR, Arden JB, eds. *Principles and Practice of Clinical Electrophysiology of Vision.* St. Louis: Mosby Year Book; 1991:537–543.
28. Kellner U, Wissinger B, Tippmann S, Kohl S, Kraus H, Foerster MH. Blue cone monochromatism: clinical findings in patients with mutations in the red/green opsin gene cluster. *Graefes Arch Clin Exp Ophthalmol*. 2004;242:729–735.
29. Michaelides M, Johnson S, Simunovic MP, et al. Blue cone monochromatism: a phenotype and genotype assessment with evidence of progressive loss of cone function in older individuals. *Eye*. 2005;19:2–10.
30. Verrelli BC, Tishkoff SA. Signatures of selection and gene conversion associated with human color vision variation. *Am J Hum Genet*. 2004;75:363–375.
31. Crognale MA, Fry M, Highsmith J, et al. Characterization of a novel form of X-linked incomplete achromatopsia. *Vis Neurosci*. 2004; 21:197–203.
32. Berson EL, Sandberg MA, Maguire A, Bromley WC, Roderick TH. Electroretinograms in carriers of blue cone monochromatism. *Am J Ophthalmol*. 1986;102:254–261.
33. Weiss AH, Biersdorf WR. Blue cone monochromatism. *J Pediatr Ophthalmol Strabismus*. 1989;26:218–223.
34. Gobel W, Hartmann F, Haigis W. Determination of retinal thickness in relation to the age and axial length using optical coherence tomography [in German]. *Ophthalmologe*. 2001;98:157–162.
35. Schaudig UH, Glaefke C, Scholz F, Richard G. Optical coherence tomography for retinal thickness measurement in diabetic patients without clinically significant macular edema. *Ophthalmic Surg Lasers*. 2000;31:182–186.
36. Ishikawa H, Stein DM, Wollstein G, Beaton S, Fujimoto JG, Schuman JS. Macular segmentation with optical coherence tomography. *Invest Ophthalmol Vis Sci*. 2005;46:2012–2017.